Scaling relations for hadron continuum scattering from carbon

R. J. Peterson
Department of Physics, University of Colorado, Boulder, Colorado 80309-0390, USA
(Received 28 December 2011; revised manuscript received 16 March 2012; published 22 June 2012)

Five scaling relations familiar from analyses of inclusive electron scattering spectra on complex nuclei are applied to 65 inclusive continuum spectra of protons, positive kaons, and pions incident upon carbon. Beam energies range from 300 MeV to 18.3 GeV with momentum transfers such that the conditions for quasifree scattering are met, similar to those for many electron scattering analyses. Several very strong assumptions need to be made to apply these scaling analyses to hadrons, and so the requirement that these spectra come into agreement under a scaling analysis is a severe test of these assumptions. Scaling is found in the sense that the responses of four of the five systems considered do agree over a significant range of momentum transfers for the three hadron species over a wide range of beam energies. Responses other than those for quasifree scattering destroy the validity of scaling systems for hadrons at large angles or momentum transfers or high beam energies.

DOI: 10.1103/PhysRevC.85.064616 PACS number(s): 25.40.Ve, 25.80.Ls, 25.80.Nv

I. SCALING

Scaling relations for inclusive (single-arm) continuum-scattering spectra from nuclei in which two or more observable variables are combined to present those spectra in terms of a new single variable have been a valuable tool using continuum (e,ex) electron scattering data to infer important aspects of nucleons within complex nuclei [1]. The basis of the success of these schemes is the well-known, incoherent, and not strong interaction of the intermediate-energy electron beam with each struck nucleon in the complex nucleus target, enabling the validity of the quasifree and impulse approximation conditions [2]. In contrast, spectra from intermediate-energy hadron continuum scattering can meet the conditions for quasifree scattering but do not meet the conditions for use of the impulse approximation due to the large cross sections [2], and it is not *a priori* evident that hadron continuum spectra should scale in the ways observed for electrons. Moreover, the fundamental hadron-nucleon scattering used in scaling models has a wide range of interactions, not simple, depending upon the beam particle and its energy, a cross section so large as to make scattering from only one nucleon at a time unlikely, and cross sections that are possibly dependent upon the density within the nucleus where the hadron interacts. The use of scaling relations which have been demonstrated to be valid for electrons to compare intermediate-energy hadronic spectra can be expected to test the validity of several strong assumptions for hadronic interactions.

If hadronic scaling can be demonstrated, even over some limited range, we would gain a valuable tool to interpolate yields from reactions from previous data, most importantly for (p,nx) results where experiments are very difficult. Furthermore, there are six interactions to be observed in the nucleonic response to an external probe (two isospins and three spin responses—nonspin, transverse spin perpendicular to the axis of the three-momentum transfer q, and longitudinal spin, parallel to q). If means are found to understand hadronic scaling, the wealth of reactions which are experimentally accessible would enable a wider breadth of nucleonic spin- and isospin-response studies beyond the two (nonspin charge and nearly isovector transverse spin magnetic) available with electrons. Since the strengths of the hadronic interactions within a nucleus that determine the response to an external probe vary differently with momentum transfer [3], scaling studies could test the role of these interactions within nuclei. Differences in the relative strengths of isoscalar and isovector interactions with a range of hadron beams also create a test of the hypotheses behind scaling. Single charge exchange reactions (SCX) will be purely isovector, while scattering without charge exchange (NCX) of protons, K^+, and pions is mostly isoscalar. The relative isoscalar singly differential hadron-nucleon cross sections change little with hadron beam energy as will be shown in Sec. VIII, whereas the relative isovector strength decreases strongly as the hadron beam energy increases. This paper will consider only NCX reactions, and Sec. VIII will compare scaling observations with these isospin trends.

This paper applies five scaling systems that have been used for electron scattering analyses to a wide range of hadronic beams on one nucleus, carbon. Since few complete spin-dependent cross section measurements are available, only the total responses are used. Data from high-quality inclusive spectra of hadron beams of pions, positive K mesons, and protons will be used at beam energies from 300 to 18 300 MeV. At small momentum transfers, the conditions for quasifree scattering are not met, and at large angles or momentum transfers the hadronic spectra are dominated by products resulting from multiple interactions or pion production. It is thus expected that hadronic-scaling relations will only be valid over some restricted range of energy loss ω and three-momentum transfer q. One goal of this paper will be to determine the limits of valid scaling relations for hadrons, including seeking indications of isoscalar collective enhancements of the scaling responses at lower momentum transfers [3]. The data to be considered from Refs. [4–14] are listed in Table I, totaling 65 hadron spectra for carbon.

The five scaling relations to be used below arise from different assumptions, but all arise from an impulsive quasifree

TABLE I. The sources of the measured inclusive doubly differential hadron-carbon cross sections used for the present paper are listed. The neutron-proton average free-space beam-nucleon total cross sections are listed as are the $A_{\rm eff}$ used in the scaling computations with in-medium total cross sections 70% of those in free space. Systematic uncertainties are given for each citation, and only statistical error bars are shown in the data plots of this paper.

Beam energy (MeV)	Beam momentum (MeV/c)	q range (MeV/c)	σ_t (mb)	$A_{\rm eff}$	Uncertainty (%)	References
$500\pi^+$, π^-	624	312–620	25.76	5.161	10	4
$653\pi^-$	780	350,500	28.05	4.894	11	5
$722\pi^-$	850	350,500,550	27.31	4.974	11	5
$820\pi^-$	950	350–650	38.17	3.765	11	5
$870\pi^-$	1000	350,500,650	42.08	3.447	11	5
367 K^+	705	384,480	13.75	5.33	11	6
300 protons	808	407–781	29.84	4.695	10	7
392 protons	942	325–730	29.68	4.713	10	7
400 protons	954	482,199–450	29.76	4.803		8,9
420 protons	982	375	30.03	4.675		10
558 protons	1165	410–1015	35.11	4.161	10	11
795 protons	1457	280–740	42.31	3.528	4.3–6.2	12
1014 protons	1711	406–603	42.51	3.512	13	13
18 300 protons	19 200	711–1500	40	3.72	11–15	14

mechanism with one-and-only-one interaction between the projectile and one bound nucleon. The conditions for such an impulsive quasifree mechanism are defined in Chap. 11 of Ref. [2], with the important feature of factoring the scattering mechanism from the nuclear structure as the response. Such single scattering is expected to be restricted to small scattering angles, which is consistent with a Glauber or eikonal model to count the number of nucleons scattered from, once and only once. A related model of quasifree scattering has been applied to large-angle continuum spectra for protons on heavy nuclei with the conclusion that instances of scaling for these few cases are only accidental [15]. The present paper will emphasize forward scattering.

It has been emphasized that it is the approach to scaling with increasing momentum transfer which reveals the dynamics behind scaling [16], and for hadrons, these dynamics are not simple. Interpolations of the responses at fixed values of the five scaling variables will be plotted against momentum transfer to compare a wide range of hadron-scattering data to seek scaling among the several beams. Also, scaling trends with fixed momentum transfer are examined as the hadron beam energy is changed.

II. METHODS

The most important assumption for all cases in the present paper is that of quasifree scattering from bound nucleons with the use of the impulse approximation assumed, even though not formally valid. Under some range of kinematic conditions [2], the collision of the incident hadron on one-and-only-one bound nucleon can be incoherent. The incident and exit beam momenta must be large compared to the bound nucleon kinetic and potential energies ($k \gg 290$ MeV/c). The momentum transfer also sets a momentum scale larger than the range of intranuclear interactions. These conditions lead to the expectation that scattering can be quasifree for laboratory three-momentum transfers q above about 450 MeV/c and beam and ejectile energies above about 400 MeV. Under these conditions, the doubly differential cross section factorizes [8,17]. In addition, Pauli blocking will influence the scattering for momentum transfers less than twice the Fermi momentum. Here, the Fermi momentum $k_{\rm F}$ for carbon is taken as 228 MeV/c [18]. Since it is the goal of this paper to explore the limits of scaling, beam energies and momentum transfers are taken over a wider range than formally appropriate. The cases to be presented are listed in Table I with their ranges of q. Studies of quasifree pion scattering at lower beam energies near the Δ resonance [19] are not considered here since those low energies are far from consistent with the approximations used in this paper, and other reaction models are more appropriate.

A second assumption for all cases is in the calculation of the number of nucleons within carbon that are struck elastically once and only once, which limits the reaction to the nuclear surface [17]. The Glauber model used here [20] uses the distribution of nucleons within carbon taken from Ref. [21] and in-medium projectile-nucleon total cross sections. These are taken as 70% of the free-space total cross sections for protons and pions on nucleons [22], a change that gives better scaling over a wide range of nuclei [23] and has been anticipated on theoretical grounds [24]. In the present paper, the same 70% of free-space total cross sections [25] is applied for the analysis of K^+ quasifree spectra, although there is other evidence that these projectiles encounter "swollen nucleons" within nuclei [26]. This number $A_{\rm eff}$ changes with the choice of projectile, ranging here for carbon from 3.412 for 1014 MeV protons to 5.161 for 500 MeV pions and 6.79 for 367 MeV K^+; comparisons of a range of beams by scaling among beams are a test of this model. This Glauber approximation is valid for small scattering angles, although used here out for quite large angles. Recent papers have shown that the eikonal or Glauber approximation is valid for proton energies down to 250 MeV [27], below the incident energies considered for the present paper.

Other than at the energy loss corresponding to scattering from a free nucleon, the hadron-nucleon scattering is off-shell. The optimum frame method [28] is used to compute hadron-nucleon elastic differential cross sections at other energy losses. The off-shell method calls for evaluating the on-shell differential cross section at different energies and angles [29]. Since the free-space π-nucleon cross sections show resonances not seen in π-carbon total cross sections [30], an average is taken of cross sections at the off-shell energy and 18 MeV above and below that value to average over the internal motions that would broaden resonances in carbon. For energy losses ω greater than those for free scattering, the variation in these computed off-shell singly differential cross sections can be large, and this unreliability sets a limit on the range over which scaling is considered in this paper.

Data presented in scaling formats in this paper include cases where the kinematic conditions for the quasifree and Glauber assumptions are not valid. These and the other assumptions and parameter choices are tested by presenting the scaled responses for carbon to see which cases do indeed scale. In the expressions below, the momentum transfer q is always replaced with the effective momentum transfer to include the beam and carbon charges [$q_{\rm eff} = q(1 \pm 4Ze^2/3Tr_0A^{1/3})$ [31] with $r_0 = 1.2$ fm and T as the projectile kinetic energy, and the energy loss ω is replaced by ω-recoil-20 MeV to include the nucleon binding energy [18,32] and the recoil energy of an elastically scattered hadron from carbon for each spectrum. The parameter ω is thus the excitation above nucleon binding. The free nucleon mass is M in these expressions. The momentum transfers q cited for examples below are for free hadron-nucleon scattering in each case save for the data of Ref. [5] where events were assembled in bins of fixed q.

Five scaling systems are presented with energy bins ω from the data approximately equal to the resolution of each experiment.

The first scaling system is y scaling as applied to electron scattering [33] by using a variable y as the least component of the internal momentum of the struck nucleon (the component in the direction of the three-momentum transfer q) to give scattering with an observed energy loss ω [1]. The y-scaling variable for an infinitely heavy nucleus is

$$y = \sqrt{[\omega(\omega + 2M)]} - q. \tag{1}$$

Scattering from a bound nucleon at rest is found at $y = 0$. A correction for the recoil of the final nucleus less the one removed nucleon as used in Ref. [34] is not included since all five variables use the same definition of ω, which includes carbon elastic recoil. Data are plotted as their y-scaling responses by

$$F(y) = d^2\sigma/d\omega\, d\Omega\; q/d\sigma/d\Omega\; A_{\rm eff}\sqrt{[M^2 + (q + y)^2]}. \tag{2}$$

Here, the kinematic factor is not just that to transform the bins of energy loss into bins of y [where q in the numerator would be replaced by $(q + y)$], but for the scaling variables below, the kinematic factors are simply those for the change in variable from the experimental energy loss, including the binding parameters to compute ω. y-scaling responses as presented here are thus not on the same footing as the other four responses, which use exactly the adaptation due to the change in variable. This y-scaling usage is taken as parallel to the large body of electron-scattering analyses. Hadronic y-scaling NCX responses for a range of beams have been published for many nuclei in Ref. [35] with comparisons to electron scattering.

The second scaling system is that due to West, derived from conservation of energy and momentum on the mass shell, to yield a variable [16,36],

$$w = (2M\omega - q^2)/2Mq. \tag{3}$$

Scattering from a bound nucleon at rest is found at $w = 0$. The scaling response derived from measured doubly differential cross sections is

$$W(w) = q\; d^2\sigma/d\omega\; d\Omega/d\sigma\;/d\Omega\; A_{\rm eff}. \tag{4}$$

Another scaling variable is that due to Bjorken, with the variable x (often called $x_{\rm B}$) as the fraction of the total nuclear momentum held by the one struck nucleon in the infinite momentum limit; this system has been used for nucleonic responses in carbon observed by electron scattering [37], and ratios of Bjorken-scaling responses for electrons have been used to infer effects of correlations among nucleons [38],

$$x = Q^2/2M\omega = (q^2 - \omega^2)/2M\omega. \tag{5}$$

Scattering from a bound nucleon at rest is found at $x = 1$. Bjorken responses are plotted as

$$B(x) = d^2\sigma/d\omega\; d\Omega\; 2M\omega^2/d\sigma/d\omega\; A_{\rm eff}\,(q^2 + \omega^2). \tag{6}$$

Bjorken responses have been given for many nuclei for NCX reactions [39] for a range of hadronic beams, particularly for a search for short-range correlations. Note that the energy loss ω occurs in such a fashion as to make the Bjorken variable and its response very sensitive to the 20 MeV separation energy parameter in ω at low energy losses.

The Nachtmann scaling variable has been applied to continuum electron data [1,40]. Use of this variable measuring the light cone momentum avoids scaling violations due to finite Q^2 (four-momentum transfer) corrections to Bjorken scaling. This variable uses

$$\xi = 2x/(1 + \sqrt{[1 + 4M^2x^2/Q^2)}] = (q - \omega)/M, \tag{7}$$

with responses defined as

$$X(\xi) = d^2\sigma/d\omega\; d\Omega\; M/d\sigma/d\Omega\; A_{\rm eff}. \tag{8}$$

The modest momentum transfers considered in this paper are insufficient to meet the conditions where the Nachtmann variable is expected to be valid [1].

A relativistic scaling variable has been defined [34,41] and has been widely used to demonstrate scaling effects for electron spectra [42–45],

$$\psi = 1/\sqrt{\xi_F}(\lambda - \tau)/\sqrt{\{(1 + \lambda)\tau + \kappa\sqrt{[\tau(1 + \tau)]}\}}, \tag{9}$$

with $\xi_F = \sqrt{(1 + \eta_F^2)} - 1$, $\eta_F = k_F/M$, $\tau = \kappa^2 - \lambda^2$, $\lambda = \omega/2M$, and $\kappa = q/2M$. Scattering from a bound nucleon at rest is found at $\psi = 0$. With the current use of a separation

energy to define ω, many papers call this variable ψ' [33]. The relativistic response is shown here as

$$\Phi(\psi) = d^2\sigma/d\omega\, d\Omega\, d\omega/d\psi/d\sigma/d\Omega\, A_{\rm eff}, \qquad (10)$$

with the transformation $d\omega/d\psi$ computed numerically.

Comparisons of scaling from a range of nuclei require inclusion of their different Fermi momenta, presented as the scaling variable $Y = y/k_{\rm F}$. Hadron continuum scatterings for this superscaling system [34,42] have been presented elsewhere for many nuclei [35].

The assumption of one-and-only-one hadron-nucleon elastic collision is violated when that collision produces a new pion. This effect is seen clearly in comparisons of electron charge and transverse magnetic excitations [34] where only the isovector transverse scattering is allowed to create a pion. Hadron SCX thus sees this effect more strongly than NCX reactions at large energy losses since most of the NCX response is isoscalar.

Hadron scattering (NCX) with protons, K^+, and pions at a range of energies contains both isoscalar and isovector components; the cases in Table I are predominantly isoscalar as discussed in Sec. VIII. Proton continuum spectra may be driven by spin terms. A few experiments, both NCX and SCX, have used spin observables to separate nonspin, longitudinal spin, and transverse spin responses [10,46–48], but these are not shown here. Spin zero pion and kaon responses can have spin transfer terms only in the transverse sense.

Inclusive doubly differential cross sections were taken from published tables when available and were measured from graphs in other cases. Uncertainties shown here include only the given statistical uncertainties of the data used. Each experiment also has some systematic uncertainty, given in the original sources as listed in Table I. Examples of hadron doubly differential cross-sectional spectra from carbon at momentum transfers q near 500 MeV/c are shown in Fig. 1 with an energy-loss scale equal to the measured laboratory energy loss minus a 20 MeV binding energy and elastic recoil as used for calculation of the scaling variables [4–6,8,12,13]. It is seen that each spectrum shows a maximum near the free-nucleon energy loss at $q = 500$ MeV/c of 133 MeV and that the maxima vary in magnitude by a factor of 7 due to differences in $A_{\rm eff}$ and in the driving hadron-nucleon singly differential cross sections. Not shown in Fig. 1 are the doubly differential cross sections for the scattering of 19.2 GeV/c ($T = 18.3$ GeV) protons at the slightly higher momentum transfer of 711 MeV/c with a peak cross section of 3300 μb sr^{-1} MeV^{-1} [14]. Scaling agreement among such a range of magnitudes will be a demonstration of the validity of the strong assumptions described above.

Also shown for the plots below are the scaling responses expected for a nonrelativistic Fermi gas (NRFG) with $k_{\rm F} = 228$ MeV/c, simply a parabola of unit area in $F(y)$. A similar curve for a relativistic Fermi gas [34,42] is compared to measured responses $\Phi(\psi)$. It is the differences from this simple model that are of greatest interest as in the case for electron scattering. In the plots of responses as a function of momentum transfer q below these NRFG responses are used for comparison, which include a Pauli-blocking factor [49]. Also shown are expectations for Pauli blocking in a slab model [17] as the dashed curve. The two models show very similar blocking with momentum transfer.

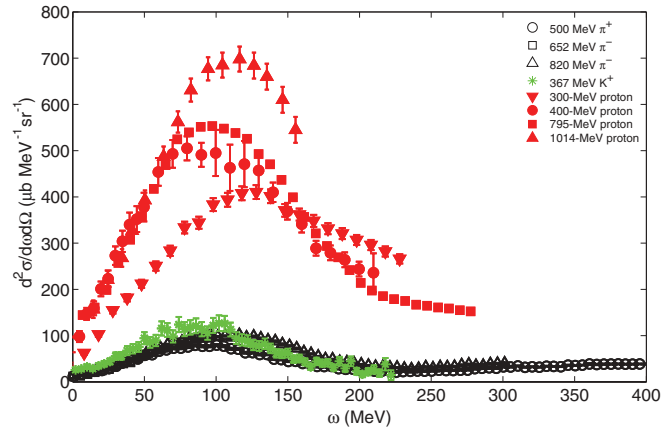

FIG. 1. (Color online) Inclusive hadron continuum spectra from carbon at momentum transfers q near 500 MeV/c are shown using the measured energy loss minus a 20 MeV binding energy and elastic recoil. Data are shown for three pion energies (500 MeV [4], 652, and 820 MeV [5]), one K^+ energy (367 MeV) [6], and four proton energies—300 MeV [7], 400 MeV [8], 795 MeV [12], and 1014 MeV [13]). Scattering from a free nucleon at $q = 500$ MeV/c would find an energy loss of 133 MeV. Not shown are the doubly differential cross sections at $q = 711$ MeV/c for 18.3 GeV protons with a maximum of 3300 μb sr^{-1} MeV^{-1} [14].

III. *y* SCALING

For y scaling of the "first kind" to be valid, spectra from a given beam and target nucleus should transform into a single pattern for all angles or momentum transfers [42].

Scaling of the first kind in the variable y defined by Eq. (1) has been demonstrated for inclusive electron scattering [1] and, through its relativistic extension, has been used as a source of information on dynamical features of nucleons within nuclei [34,42–45]. The methods and parameters described in Sec. II have been used to transcribe the 950 MeV/c (820 MeV) pion [5] and 795 MeV proton NCX [12] inclusive spectra for carbon into the y-scaling format in Fig. 2 with low energy losses to the left. The pion momentum transfers range from 350 to 650 MeV/c, and the proton data cover q from 331 to 738 MeV/c. These two experiments were designed to study continuum scaling features and covered a good range of momentum transfer, ranging from values below the validity of the quasifree conditions to well above that standard. The NRFG expectation is a simple parabola, shown for reference. Except for the pion data at $q = 650$ MeV/c, these responses peak near $y = 0$, the locus of free scattering. Both data sets are above the NRFG parabola. Figure 3 shows data for lower proton energies, 300 MeV in the upper panel [7] and 392 MeV [7] and 400 MeV [9] in the lower panel. Angles range from 12° to 75°. Except for the data at 75°, these data are similar to one another and to the higher-energy data of Fig. 2 over a wide range, especially at negative values of y. Other data over a range of angles for other hadrons show similar trends. Responses at positive y increasingly exceed

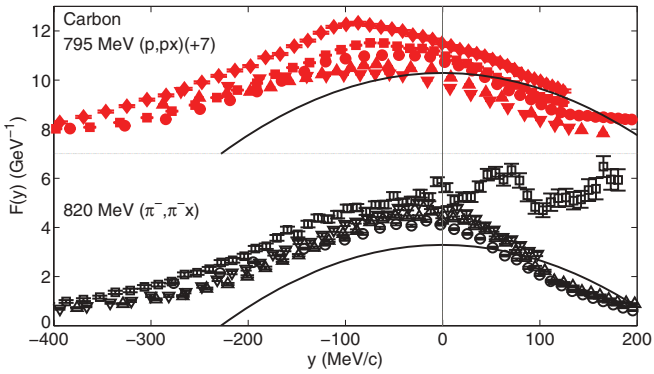

FIG. 2. (Color online) Scaling of the first kind would demand that responses not change with momentum transfer. Data from two papers on carbon with q ranging from 331 to 738 MeV/c [5,12] are shown in the y-scaling format of Eqs. (1) and (2). A NRFG gives a parabolic response in this variable, and the vertical line shows the value of $y = 0$ for free scattering. The proton data are in solid red, and the pion data are in open black points in this and other figures. Responses near $y = 0$ increase with increasing angle or momentum transfer for both beams.

the NRFG curve at larger momentum transfers as the energy losses allow pion production and other nonquasifree processes. This effect is also noted in transverse electron scattering [34]. Scaling of the first kind is followed for 65 hadron spectra over a wide range of momentum transfers for negative values of y, in that the scaled data are all very similar. Sec. VIII includes comparisons.

A comparison of spectra with momentum transfers near 500 MeV/c for a range of proton, K^+, and pion energies shows excellent NCX y scaling in Fig. 4, each with a peak near $y = 0$. Their agreement in the range of the NRFG indicates that the scaling assumptions are valid by including the optimum frame singly differential cross sections, which change over the range of negative y by 20% for protons and 50% for pions over the energy ranges of the data shown. This has been called "scaling of the third kind" [35] in which scaling is noted for a single nucleus over a limited range of momentum transfer for all hadrons. Agreement among the hadron beams is better

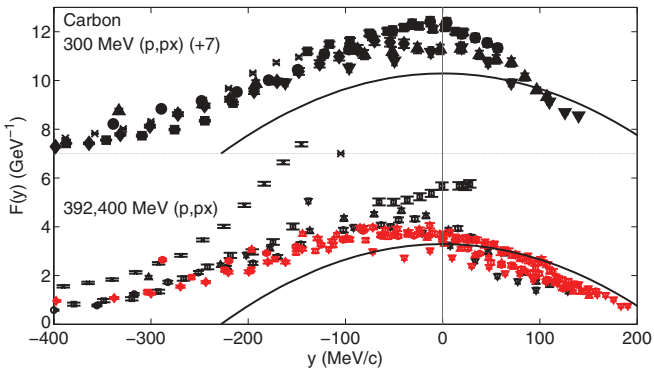

FIG. 3. (Color online) The same as Fig. 2 but for lower-energy proton beam energies. Data in black at 300 and 392 MeV are from Ref. [7] from 20° to 75° and red points at 400 MeV are from Ref. [9] from 12° to 28°. The curve again shows the expectation for a NRFG.

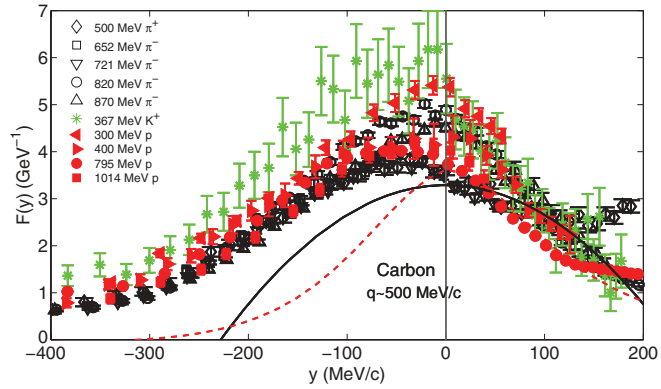

FIG. 4. (Color online) Hadronic spectra from carbon with q near 500 MeV/c are shown in the y-scaling format with a solid curve showing the parabolic response expected for a NRFG. In this range of momentum transfers, good scaling is found at quite negative values of y for ten different beams from seven different experiments with three different hadron beams. Proton data [8,12,13] are in red, pion data [4,5] are in black, and K^+ data [6] are in green. Also shown as the dashed curve is the "universal" fit to electron responses used in Ref. [43].

at more negative y. This is the region of greatest interest for nuclear dynamics.

Also shown in Fig. 4 is the universal curve of electron scattering responses [43], adapted to the Fermi momentum appropriate for carbon. These electron responses change little with momentum transfer q. The hadron responses at negative values of y consistently exceed the curve, which is fit to electron data including large momentum transfers. This excess is discussed in Sec. VIII.

At a higher q range from 600 to 750 MeV/c, an extended range of y-scaling responses for carbon is shown in Fig. 5. Responses for pions and protons of nine beam energies as far

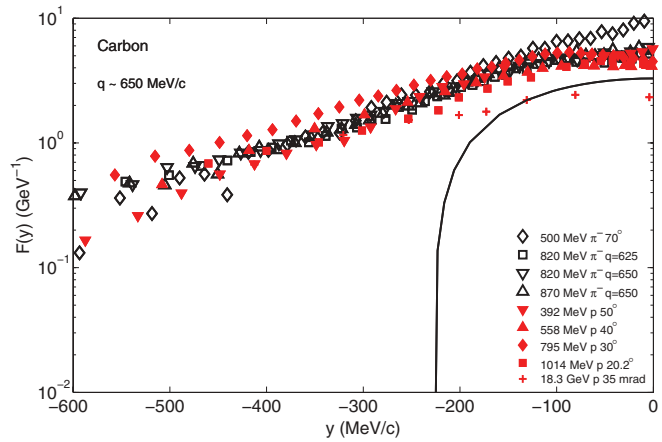

FIG. 5. (Color online) Hadronic spectra from carbon for reactions with q from 600 to 750 MeV/c are shown on a logarithmic scale for negative values of y. The curve shows the expectation of a NRFG. Good concurrence is found for these data sets at very negative values of this scaling variable. Colors are used as in the previous and following figures.

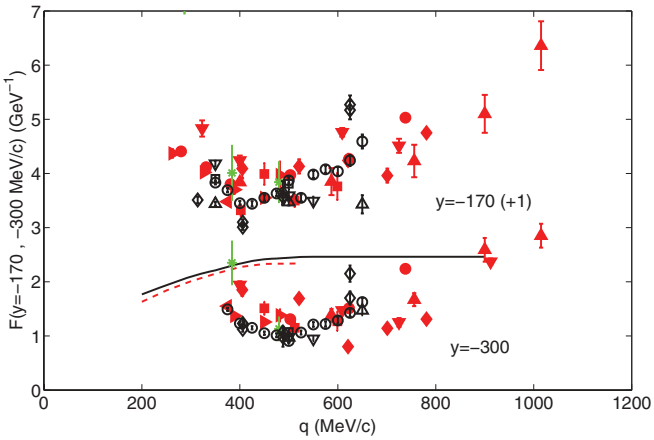

FIG. 6. (Color online) Values of the y-scaling responses for carbon interpolated for $y = -170$ and $y = -300$ MeV/c are plotted for a range of momentum transfers q. The scattering responses are tightly clustered and rise smoothly with q from a minimum, near $q = 400$ MeV/c at $y = -170$ MeV/c and near $q = 500$ MeV/c for $y = -300$ MeV/c. Proton data are in red, pion data are in black, and K^+ data are in green; the fitted slopes with q above $q = 500$ MeV/c for these results are found in Table II; average values for q between 400 and 600 MeV/c are found in Table III. The solid curve shows the expectation at $y = -170$ MeV/c of the Pauli-blocked NRFG; $y = -300$ MeV/c is beyond the range of this simple expectation. The dashed curve shows the prediction for the slab model of Ref. [17] for $y = -170$ MeV/c. These curves have been incremented by one as the data.

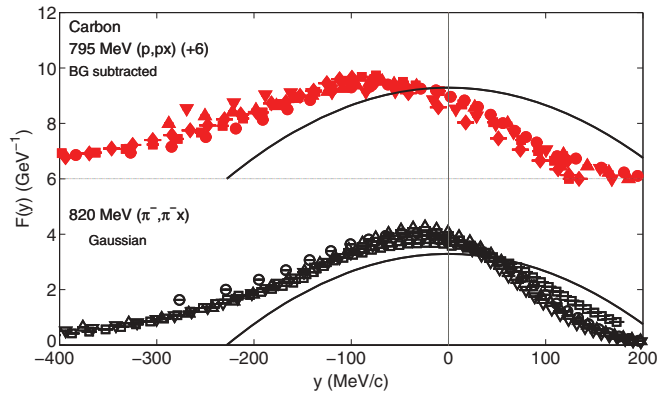

FIG. 7. (Color online) Backgrounds (BG) as described in the text have been subtracted from the carbon continuum spectra for 795 MeV protons [12], and an asymmetric Gaussian fit with a linear background to the 820 MeV pion data [50] was made to yield the y-scaling responses shown for carbon. The curve shows the expectation for a NRFG. These responses are more similar to one another, showing better scaling of the first kind than is noted in Fig. 2.

as 18.3 GeV agree quite well out to values of y far from that allowed by the NRFG curve shown.

Responses near $y = 0$ and for positive y include events from pion production not included in the scaling analysis as deduced in Ref. [34].

The NCX y-scaling responses interpolated for $y = -170$ MeV/c ($\omega = 56$ MeV at $q = 500$ MeV/c) show a tight pattern with a minimum near 400 MeV/c in Fig. 6. The average value of these responses is compared to those of the other scaling schemes in Sec. VIII. At this value of $y = -170$ MeV/c, the NRFG expectation would be 1.46 GeV^{-1}.

At more negative values of y beyond the NRFG at $y = -300$ MeV/c ($\omega = 21$ MeV at $q = 500$ MeV/c), interpolated responses are also shown in Fig. 6. As at $y = -170$ MeV/c, NCX responses for hadron scattering show a tight pattern with a minimum near 500 MeV/c. The pattern is particularly smooth for the 820 MeV pion data, shown as open circles [5]. This clustering of responses shows scaling of the third kind as similar for all hadronic probes [35], even though scaling of the first kind defined in Ref. [45] is not found since the responses do depend upon the momentum transfer as seen in Fig. 2. The scatter of data points and slopes with q is compared to trends from the other scaling systems in Sec. VIII.

At positive values of y, pion production is expected to give a background of events not expected to scale by the models used in this paper. A linear background for the 795 MeV data on carbon [12] was estimated by one point at the largest energy loss and zero at an outgoing energy of 775 MeV for 13°, 15°, and 20° and 750 MeV for 25° and 30°. The y-scaling responses for these subtracted spectra are shown in Fig. 7. For the 820 MeV π^- carbon data, Fig. 7 also shows the results of a Gaussian fit to the doubly differential cross sections with a subtraction of low-lying discrete peaks and a linear background [50]. This is the peak shape suggested from inclusive electron scattering spectra in Ref. [51]. These data agree better among themselves than the cases with a background in Fig. 2 and are near the NRFG curve near $y = 0$. Maxima of the pion response peak near $y = 0$, but those for 795 MeV protons peak at negative y. Deviations from scaling of the first kind are thus found to be largely due to nonquasifree events, strongest at larger scattering angles.

IV. WEST SCALING

Figure 8 shows the West scaling responses $W(w)$ for carbon defined by Eqs. (3) and (4) for two NCX experiments that cover a wide range of momentum transfers [5,12]. In both cases, the responses $W(w)$ rise with increasing angle or momentum transfer as also noted for the y variable. Other reactions with fewer cases are quite similar. The curve shows the NRFG expectation for the West response for $q = 500$ MeV/c.

The scattering (NCX) 795 MeV proton data are for q from 331 to 738 MeV/c. These data peak at the maximum of the NRFG curve and agree among themselves at negative w only for the smallest angles with q up to about 400 MeV/c. In contrast, the pion data peak nearer $w = 0$ with responses rising with q from 350 to 650 MeV/c. The responses at negative w agree up to about 550 MeV/c.

Figure 9 shows the scaling response $W(w)$ for ten continuum spectra for NCX inclusive scattering on carbon with different beams and energies at momentum transfers from 488 to 512 MeV/c as also shown for y scaling in Fig. 2 [4–6,8,12,13]. For $w < 0$ with energy losses ω less than would be found for free scattering, these all look much the same with a peak near $w = 0$, unlike the NRFG curve shown

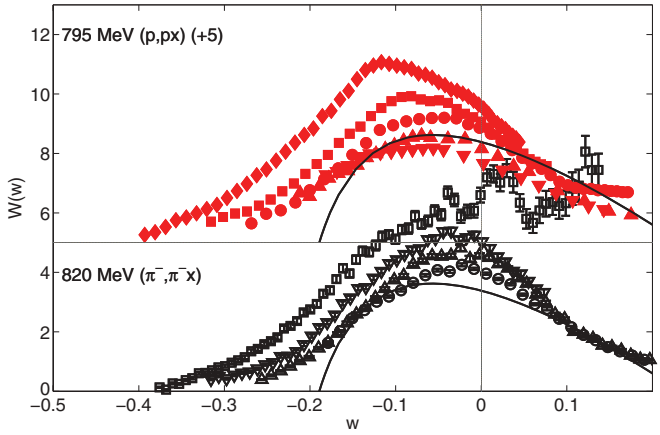

FIG. 8. (Color online) The West-scaling response defined by Eqs. (3) and (4) is shown for two series of hadronic NCX cross sections on carbon covering a range of momentum transfers from 331 to 738 MeV/c for 795 MeV protons (13°, 15°, 20°, 25°, and 30°) [12] and for q = 350, 450, 550, and 650 MeV/c for 820 MeV negative pions [5]. The proton responses are incremented by five. The responses near $w = 0$ rise for each case with angle or q. The curve is the expectation for a NRFG, and the vertical line shows the variable $w = 0$ for free scattering.

for q = 500 MeV/c. At w near zero, there is a systematic increase in this response for lower energy hadron beams. At lower energies, larger angles must be used to achieve this relevant momentum transfer, and other mechanisms enter more strongly at larger energy losses as noted from the background-subtracted results in Fig. 7.

The approach to scaling with q is demonstrated in Fig. 10 by the interpolated responses $W(w = -0.15)$ and $W(w = -0.24)$, which correspond to energy losses ω near 58 and 13 MeV at $q = 500$ MeV/c, as shown in Fig. 6 for y scaling by using data from 300 to 1014 MeV [4–8,12,13]. The NCX data in this scaling variable cluster tightly and rise smoothly with q by

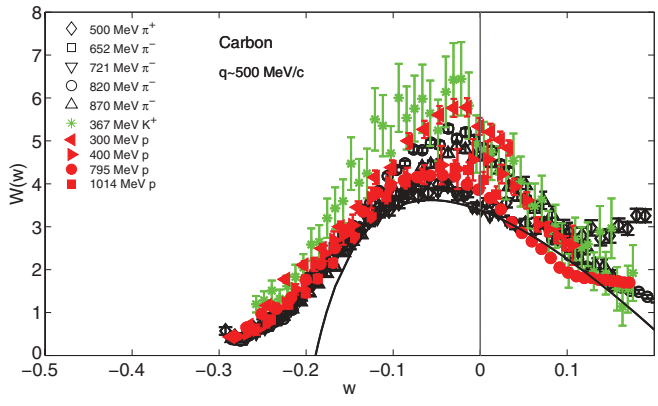

FIG. 9. (Color online) Scaling of the third kind in the West variable would be demonstrated if a wide range of hadronic beams—pions [4,5], protons [7,8,12,13], and K^+ [6]—at different beam energies were to give the same response. Here, the West scaling system is used to compare hadronic responses of carbon with q from 488 to 512 MeV/c. The curve shows the expectation of a nonrelativistic Fermi gas.

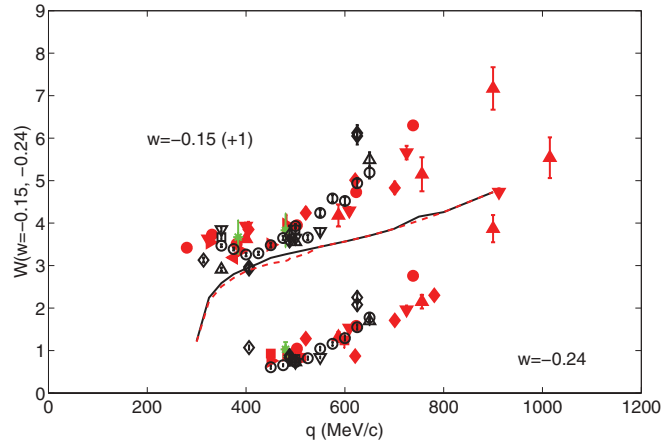

FIG. 10. (Color online) Hadronic responses of carbon interpolated for $w = -0.15$ and $w = -0.24$ are plotted against the laboratory frame free momentum transfer q for NCX responses on carbon with data for proton energies from 345 to 1014 MeV, 367 MeV K^+, and pion energies from 500 to 870 MeV. Sources of the data are listed in Table I. The curves show the values expected from Pauli-blocked NRFG and slab models for $w = -0.15$.

exhibiting scaling of the third kind as noted for the y variable. The curves shown are the West responses for the NRFG and slab models, rising with q at $w = -0.15$, similar to the data.

Comparisons of the trends with q for the several scaling variables are shown in Sec. VIII.

V. BJORKEN SCALING

The same 820 MeV pion and 795 MeV proton NCX data for carbon shown in Figs. 2 and 8 are shown in the Bjorken scaling format in Fig. 11 as calculated from Eqs. (5) and (6) with lower energy losses to the right. Over most of the range of momentum

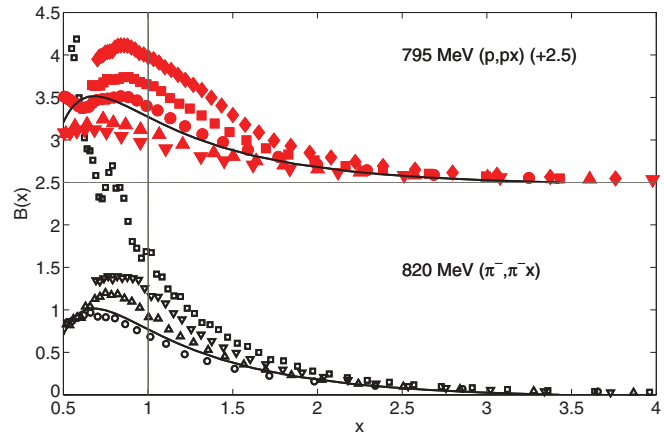

FIG. 11. (Color online) As for the previous sections, the same NCX data for pions and protons on carbon are shown in the format of the Bjorken scaling variable, compared to a curve showing the expectation of a nonrelativistic Fermi gas. Free scattering is found at $x = 1$ and lower-energy losses are to the right. Responses near $x = 1$ rise with increasing angle or momentum transfer.

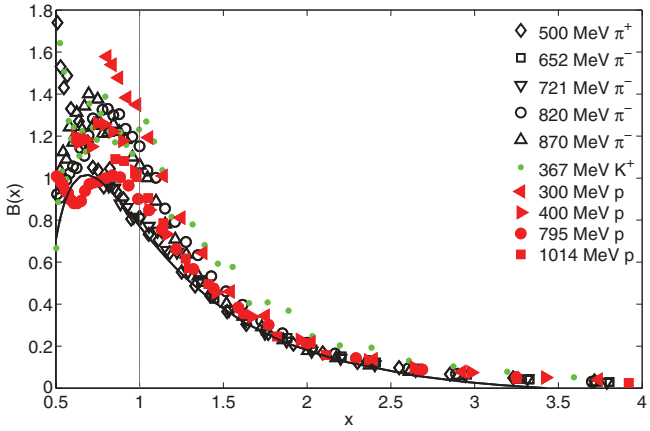

FIG. 12. (Color online) Scattering data on carbon in the Bjorken scaling format from a range of pion, K^+, and proton energies are shown for q between 488 and 587 MeV/c, compared to the Fermi gas curve. Data are as seen in Figs. 4 and 9.

transfer, these responses differ more from one another than was noted for y or West scaling, especially near the free-scattering point of $x = 1$. The data are not matched by the curve shown (derived from the NRFG), except at the lowest momentum transfers. Free scattering would be found at $x = 1$, whereas responses at larger values of this variable are suggested to arise from nuclear correlations [38]. A presentation of Bjorken NCX responses to hadrons for a wide range of nuclei is found in Ref. [39], and electron data at larger momentum transfers are found in Ref. [37].

The same wide range of ten hadron spectra for q near 500 MeV/c as used in Figs. 4 and 9 above are shown in the Bjorken format in Fig. 12. These do not agree as well as was noted for the y and West formats near $x = 1$ but are in tight agreement at larger values of x.

As shown for the other variables, the dependences of the Bjorken responses for carbon with momentum transfer are shown in Fig. 13 at fixed values of $x = 1.5$, 2.0, and 2.3. The q dependences at these values of x are very similar to

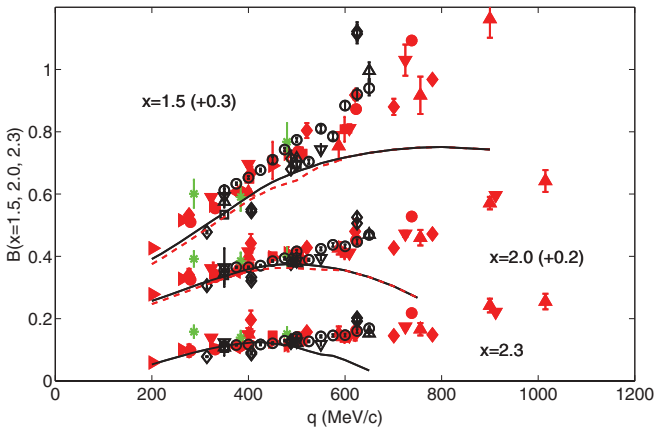

FIG. 13. (Color online) Data in the Bjorken scaling system interpolated for $x = 1.5$, 2.0, and 2.3 are compared similar to that in Figs. 6 and 10. Curves show the expectations of a Pauli blocked NRFG and a slab model at these values of x.

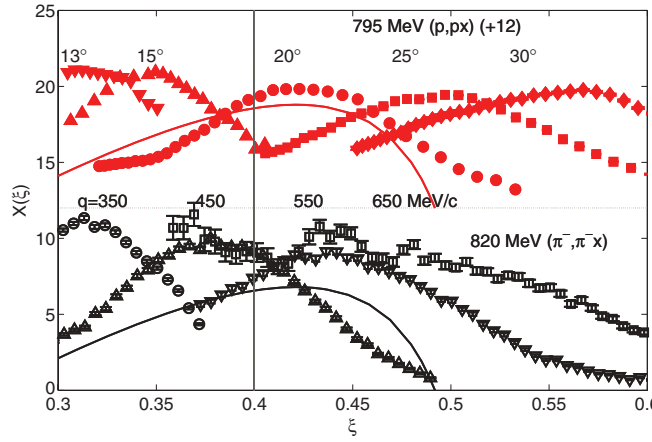

FIG. 14. (Color online) The same scattering data on carbon for pions at 820 MeV [5] and protons at 795 MeV [12] at a range of angles or q are shown in the Nachtmann scaling variable. Data show no consistent scaling patterns and little resemblance to the curve that shows the expectation for a nonrelativistic Fermi gas at $q = 500$ MeV/c. Free scattering would be found at $\xi = 0.3998$ for $q = 500$ MeV/c.

those expected up to moderate values of q but continue to rise beyond the curves at larger momentum transfers. The slopes of these rises will be compared in Sec. VIII.

VI. NACHTMANN SCALING

Figure 14 shows carbon response data in the Nachtmann scaling variable for 795 MeV (p,px) [12] and 820 MeV $(\pi^-, \pi^- x)$ [5]; these are the data also used in related figures in previous sections. Responses at lower energy losses are to the right. In neither case do the data demonstrate scaling of the first kind in this scheme, with the patterns shifting to larger ξ as the momentum transfer increases, with the same maximum values of the response. The data sets, left to right, for the protons are from 13°, 15°, 20°, 25°, and 30°, and the pion data are for $q = 350$, 450, 550, and 650 MeV/c. The NRFG curve shown is for $q = 500$ MeV/c, matched well with the proton 20° data with $q = 503$ MeV/c.

For momentum transfers near 500 MeV/c, the Nachtmann responses are very similar as shown in Fig. 15 for the same data as in Figs. 4, 9, and 12. These peak near $\xi = 0.4$, similar to that expected for the NRFG response shown for $q = 500$ MeV/c.

As for the previous responses, the q dependence at a fixed value of the variable $\xi = 0.47$ of the Nachtmann responses is shown in Fig. 16. This value of ξ measures the responses at energy losses similar to those for $y = -170$ MeV/c in Sec. III. The steep rise in the NRFG reflects the sensitivity to q noted in Fig. 14; sparse data at larger q indicate the expected decrease in $X(\xi)$.

Although the Nachtmann scaling system does bring agreement near $q = 500$ MeV/c for ten hadron spectra as noted with the other variables, the strong violations of scaling of the first kind and the steep dependence of the response at $\xi = 0.47$ with q make this a less attractive system to organize hadron spectra. This observation is in contrast to the success

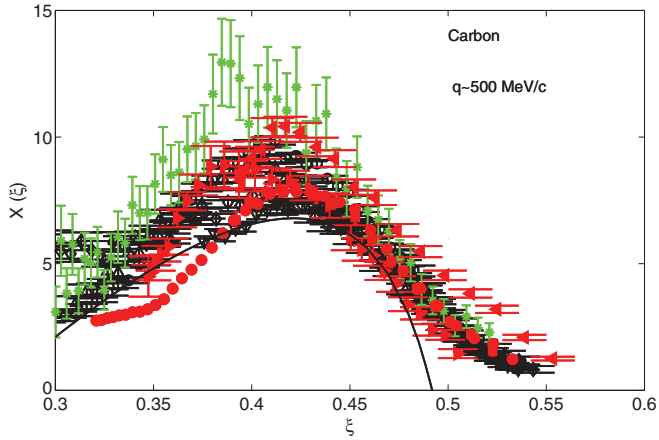

FIG. 15. (Color online) For the same restricted range of momentum transfers near 500 MeV/c used for Fig. 4, NCX cross sections on carbon for a range of beam energies for pions, K^+, and protons give a common scaling response at larger values of the Nachtmann variable ξ. The curve shows the expectation of the NRFG at $q = 500$ MeV/c.

of Nachtmann scaling for higher energy electron scattering at much larger Q^2 [40]. It has been pointed out, however, that the seemingly simultaneous y and Nachtmann scaling for electrons is accidental [52], a finding consistent with the lack of such simultaneous validity of the two schemes for hadrons.

VII. RELATIVISTIC SCALING

The expressions of Eqs. (9) and (10) are the relativistic extension of y scaling. As in Fig. 2, the two data sets, which cover a wide range of momentum transfer, are used to provide the relativistic responses shown in Fig. 17. This is the format in which to test scaling of the first kind as examined in detail for electron scattering [34,42–45]. The curve shows the expectation of a RFG. Scaling of the first kind is noted to be valid to the same level as for the y scaling in Fig. 2.

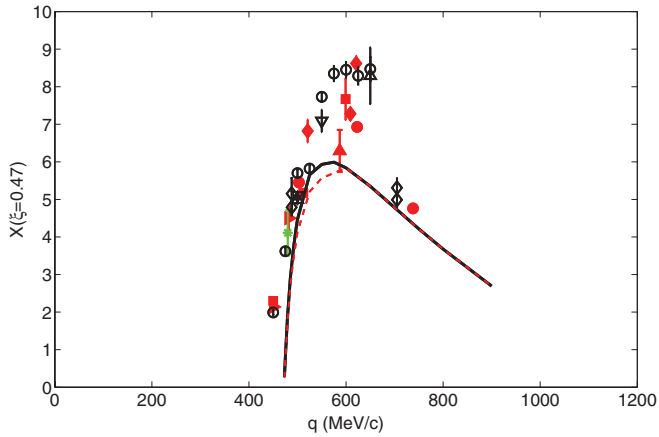

FIG. 16. (Color online) Nachtmann responses interpolated for $\xi = 0.47$ are shown for three beam species as the momentum transfer is changed. This variable greatly restricts the range of data for any one value of ξ as noted from Fig. 14. The curves show the expectation of a Pauli-blocked NRFG and a slab model (dashed line) as in the similar figures for other scaling variables.

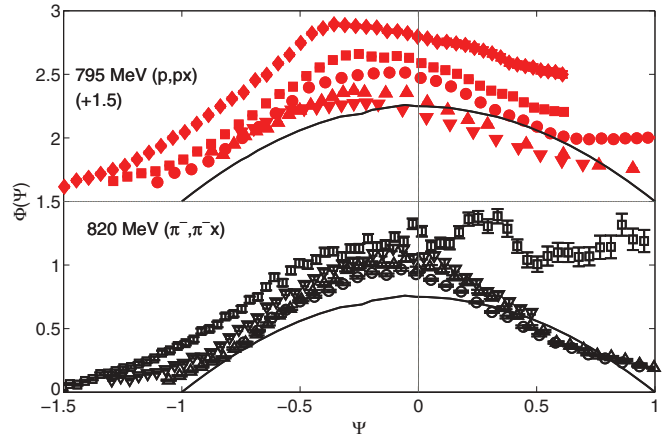

FIG. 17. (Color online) Use of the relativistic scaling variables and responses of Eqs. (9) and (10) yields the responses shown, similar to the ones in Fig. 2 [34,42]. The curve shows the expectation of a relativistic Fermi gas for carbon.

Figure 18 shows ten hadron spectra from carbon with q near 500 MeV/c as in previous sections, this time in the relativistic scaling system. Agreement with the relativistic curve is similar to that for y scaling.

As was performed for the other four scaling systems, the relativistic responses were interpolated at fixed values of the variable $\psi = -0.60$ and -1.0 to test for scaling of the first kind. Results are shown in Fig. 19. The lower value is within the range of the Fermi gas, which would there give $\Phi(\psi) = 0.48$. With Pauli blocking, this model yields the curve compared to the data for $\psi = -0.6$. Near 450 MeV/c, the data agreed better in this system than was noted in Fig. 6 in the nonrelativistic system. The very systematic data set for 820 MeV (950 MeV/c) pions shows a clear minimum, not noted from the RFG curve.

Averages and slopes with momentum transfer will be compared in Sec. VIII.

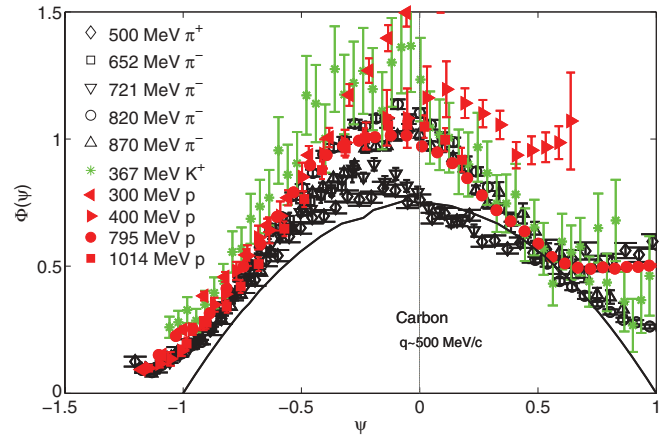

FIG. 18. (Color online) A collection of relativistic responses for q near 500 MeV/c is shown as in Fig. 4 and compared to the expectation of a relativistic Fermi gas.

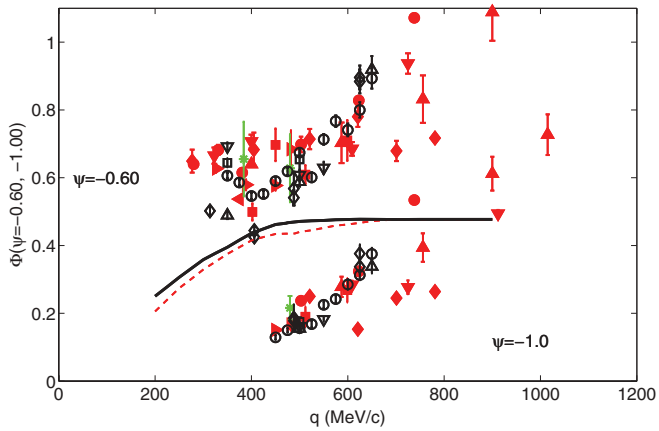

FIG. 19. (Color online) Relativistic responses interpolated at $\psi = -0.60$ and -1.0 are shown for three beam species and a wide range of angles to compare their evolutions with momentum transfer. The solid curve shows a Pauli-blocked relativistic Fermi-gas expectation for $\psi = -0.60$, whereas, the dashed curve shows a slab-model result.

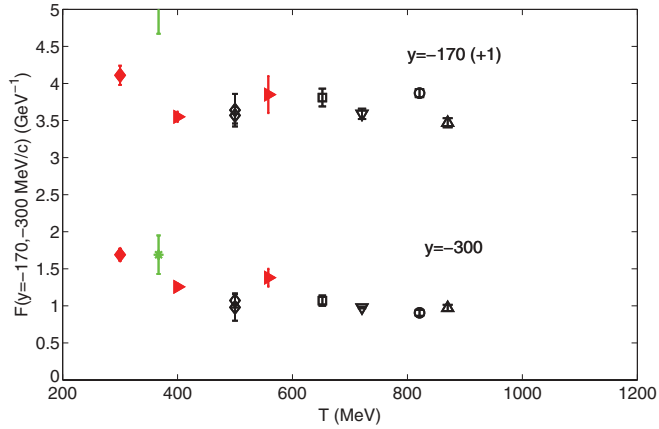

FIG. 20. (Color online) Interpolated scaling responses for q near 500 MeV/c are shown for $y = -170$ MeV/c and -300 MeV/c as a function of the beam kinetic energy. The NRFG expectation would be 1.461 GeV^{-1} at $y = -170$ MeV/c. There is little dependence on the beam energy of the hadrons driving these responses.

VIII. COMPARISONS

A. Background subtractions

The doubly differential cross sections used for this paper and their computed responses do not drop at high-energy losses as would be required for a simple single-particle response. This is largely due to pion production. The 950 MeV/c pion spectra for carbon were fit in Ref. [50] by using a double Gaussian for the quasifree peak, discrete peaks for elastic- and bound-state scatterings, and a linear background was fixed by the yield at the largest energy losses. A linear fit to the background has been used for the 795 MeV proton spectra [12]. Such an accounting for a nonquasifree background beneath the single-particle response was able to bring much closer agreement between the y-scaling responses across a range of momentum transfers in Fig. 7 as compared to the total responses in Fig. 2. It can be concluded that only for small energy losses ($y < 0$) do the hadron scaling responses of this paper measure such single-particle responses.

B. Changes with beam energy

One of the kinematic conditions for quasifree scattering is that both the incoming and the outgoing hadron energies and momenta be sufficiently high. Interpolated responses from 300 to 1014 MeV in the y-scaling system at fixed values of $y = -170$ MeV/c and -300 MeV/c are plotted for carbon in Fig. 20 for momentum transfers q near 500 MeV for three hadron species. After a slight decrease from $T = 300$ MeV, these responses are remarkably constant, indicating that the lower kinematic constraint on beam energy has been met for the present data set above a beam energy of 300 MeV.

At a proton beam energy of 18.3 GeV it has been shown that the scattering proceeds through multistep interactions except perhaps at the lowest momentum transfer of $q = 711$ MeV/c at low energy losses [53]. This is because the forward singly differential cross sections in the laboratory frame at this high energy are large and drop quickly with q as discussed in Refs. [14,35]. Responses at $q = 711$ MeV/c at 18.3 GeV are 1.81 GeV^{-1} at $y = -170$ MeV/c and 1.27 GeV^{-1} at $y = -300$ MeV/c. This beam energy is too high to be used for the determination of single-nucleon responses at $y = -170$ MeV/c.

C. Scaling of the first kind

Scaling of the first kind was noted for electron scattering responses in the y-scaling [1], relativistic [34,43], and Nachtmann [40] systems with responses independent of momentum transfer q over a wide range. Figures 2, 8, 11, 14, and 17 find this to be less true for a range of proton and pion momentum transfers, most strongly for the Nachtmann variable. Figure 6 shows that the y-scaling system gives the least change in responses at $y = -170$ and -300 MeV/c with momentum transfer, with the relativistic version of this scaling in Fig. 19 showing a similar change.

For the y-, w-, x-, and ψ-scaling systems, the slopes of the responses at fixed values of the variables shown in Figs. 4, 9, 12, 15, and 18 have been fit to see which system best meets the standard of being independent of q above 500 MeV/c. Results are listed in Table II. At moderate energy losses ($y = -170$ MeV/c, $w = -0.15$, $x = 1.5$, and $\psi = -0.60$), the fractional increase is least for the y-scaling variable. At smaller energy transfers ($y = -300$ MeV/c, $w = -0.24$, $x = 2.0$ and 2.3, $\psi = -1$), the Bjorken system agrees best with scaling of the first kind with the least slope.

In the range of momentum transfers between 400 and 600 MeV/c, the conditions for quasifree scattering are met, and the backgrounds are not yet large. The averages and standard deviations of the mean (SDOM) for 21 to 31 hadron spectra in each of the five scaling schemes are listed in Table III. These spectra come from eight discrete experiments with the systematic uncertainties of each listed in Table I. These eight experiments would lead to the expectation of a 3.9% uncertainty in the average of each response. This expectation is met or bettered at moderate-energy losses for the y-, West-, Bjorken-, and relativistic-scaling variables. At lesser energy losses ω, the Bjorken system best meets the standard.

TABLE II. Slopes of responses of carbon to hadron probes interpolated for fixed values of the observables are shown for momentum transfers above 500 MeV/c, expressed as their ratios to the average values in Table III per GeV/c. Values of y are in MeV/c; other variables and responses are dimensionless.

Response at	$y=-170$	$y=-300$	$w=-0.15$	$w=-0.24$	$x=1.5$	$x=2.0$	$x=2.3$	$\psi=-0.60$	$\psi=-1.0$
Slope (%)	1.95	2.51	3.11	8.92	3.79	2.27	1.70	2.39	4.65

Also listed in Table III are the scaling responses at the interpolated values of each of the scaling variables from inclusive electron scattering at $q = 550$ MeV/c [54]. These responses were reported as the longitudinal (charge) and transverse (magnetic) responses; the same methods as in Sec. II were used to form the interpolated values. The hadronic responses in this range of momentum transfer are generally above the charge responses and notably below the magnetic.

D. Collective effects

Isoscalar collective effects become strong below momentum transfers of about 400 MeV/c [3] and would enhance the response to an isoscalar beam interaction. The hadronic responses for q near 350 MeV/c are shown in the y-scaling format in Fig. 21. In contrast to the tight pattern of events at negative y shown in Fig. 4 for q near 500 MeV/c, these data show more scatter and a larger response, more than twice as strong near $y = -300$ MeV/c. This strengthening is the effect expected for attractive isoscalar interactions. Both figures include the universal response from electron scattering for comparison [43]. Electron scattering driven by coupling to charge sees less of any isoscalar enhancement of the responses than would hadron NCX scattering.

It might be expected that the isoscalar coupling of the three beams (proton, K^+, and pion) to carbon might differently couple to isoscalar nuclear collectivity or that this coupling might change with beam energy. Figure 22 shows the relative strength of isoscalar to total singly differential cross sections at two momentum transfers. The proton isoscalar differential cross sections have been derived from the Bystricky amplitudes within the standard free-space hadron compilation SAID [22,55], whereas the pion and K^+ differential cross sections can be deduced from combinations of computed cross sections in SAID [22].

Free-space proton beam isoscalar cross sections vary but little across the energy range of this paper, but pion isoscalar coupling increases by about 25%. The trends in the y-scaling responses of Fig. 21 show, if anything, the opposite trend at $q = 350$ MeV/c. Changes in the $\Delta S = \Delta T = 0$ proton-nucleon amplitudes within the nuclear medium are expected to be small for proton beam energies below 800 MeV [56]. Evidently, features other than beam-response coupling are more important for the differences between the responses at $q = 350$ and 500 MeV/c.

TABLE III. Average values and SDOM (in percent of the averages) are listed for scaling responses of carbon as interpolated for momentum transfers between 400 and 600 MeV/c to compare their consistencies for N examples. Values of y are in MeV/c, and responses $F(y)$ are in GeV^{-1}. Other variables and responses are dimensionless. Values expected for a NRFG are also listed, as are the interpolated electron scattering longitudinal (EEL) and electron scattering transverse (EET) responses at $q = 550$ MeV/c [54].

Response	Average	SDOM (%)	N	NRFG	EEL	EET
$y=-170$	2.76	2.7	30	1.46	2.37	6.4
$y=-300$	1.25	4.1	28	0	0.69	2.53
$w=-0.15$	2.80	3.3	30	2.26	2.60	7.0
$w=-0.24$	0.96	5.3	23	0	0.59	2.19
$x=1.5$	0.418	3.4	30	0.376	0.44	1.12
$x=2.0$	0.196	3.3	30	0.177	0.19	0.53
$x=2.3$	0.133	3.5	30	0.11	0.13	0.33
$\xi=0.47$	5.49	7.2	22	4.52	2.11	5.3
$\psi=-0.60$	0.63	2.9	31	0.485	0.57	1.53
$\psi=-1.0$	0.20	5.6	21	0	0.12	0.46

E. Momentum distributions

In the Fermi gas model, there is a simple connection between the distribution $n(k)$ of nucleon momentum (k) within a complex nucleus and the measured y-scaling response [43,52],

$$n(k) = -dF(y)/dy/2\pi y. \tag{11}$$

First differences of y-scaling responses for carbon with q near 500 MeV are shown in Fig. 23 without error bars. Statistical uncertainties lead to a wide scatter with data near

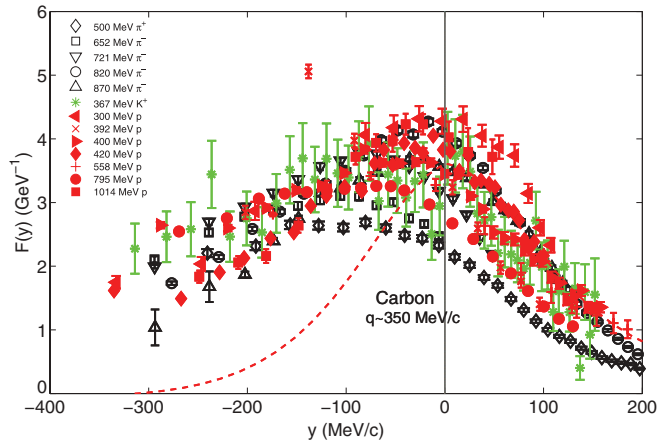

FIG. 21. (Color online) Nuclear correlations are to be sought in hadronic responses at lower momentum transfers. A wide range of hadronic y-scaling responses is shown for q between 314 and 407 MeV/c. Responses at negative y are about twice as strong as those with q near 500 MeV/c as seen in Fig. 4. The curve represents the universal electron-scattering response [43].

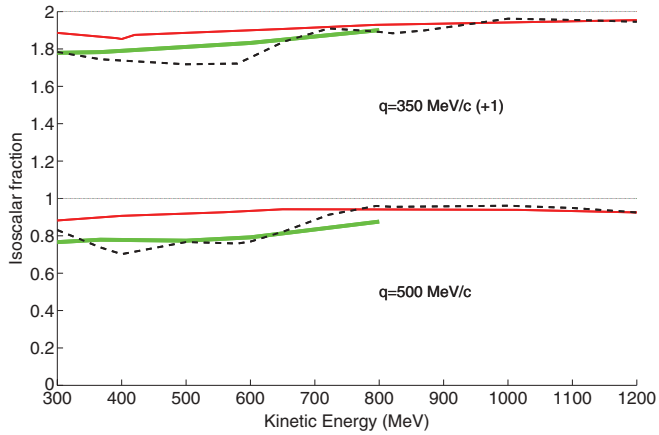

FIG. 22. (Color online) The isoscalar fractions of the singly differential cross sections used to extract scaling responses are shown for pions (dashed lines), K^+ (heavy lines), and protons (solid lines) on a symmetric nucleus as a function of the beam energy. Proton isoscalar fractions are almost constant, and those for pions rise slowly with energy.

$y = 0$ becoming very unreliable. Nonetheless, the data for ten spectra do indicate the momentum distribution sensed by hadron beams. The solid curve shows the prediction of the coherent density fluctuation model [45]; a Fermi gas would give a uniform density of 2.1 $(\mathrm{GeV/c})^{-3}$ from $k = -228$ MeV/c to zero. A semiempirical fit to momentum distributions noted by electron scattering is shown by the dashed curve [57]. The hadron beams are sensing nucleon momenta with some reliability out to $k = -400$ MeV/c and seem to be in excess relative to electron-scattering work.

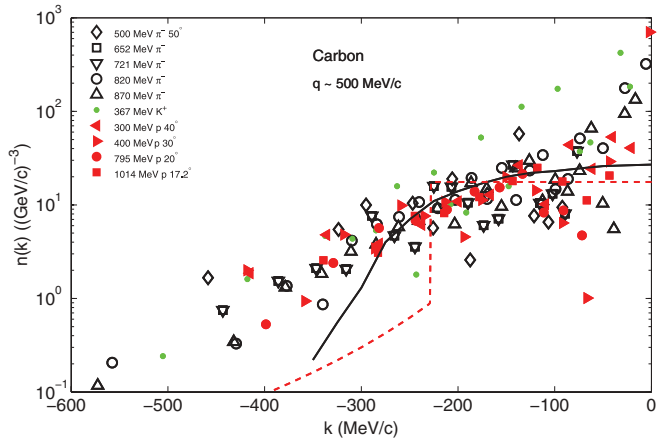

FIG. 23. (Color online) By using the expression in the text, based on a Fermi-gas model, the momentum distributions of nucleons sensed by the beams considered in this paper are shown for momentum transfers near 500 MeV/c. Error bars can be large due to differences taken between data points and are particularly large near $k = 0$. The solid curve shows one theoretical expectation, that of the coherent density fluctuation model [45], and the dashed curve shows a semiempirical fit to previous results from electron scattering [57].

IX. CONCLUSIONS

There were three goals to be addressed in this examination—do hadronic NCX continuum spectra scale over at least some kinematic range; which scaling system among five options gives the best scaling to unify hadronic data; and what are the kinematic limits for scaling of hadrons to be followed?

Since hadronic cross sections are large, several conditions that are met for inclusive electron scattering are not met here, and scaling of hadronic spectra is not to be expected, let alone agree with the responses obtained from electron data. Scaling of the first kind, independent of momentum transfer, is found for electrons [34,43] but is not noted for the range of data for 795 MeV protons [12] or 820 MeV negative pions [5] in Figs. 2, 8, 11, 14, and 17 for any of the five scaling variables. Treatment of an empirical background improved the consistency as shown in Fig. 7. Interpolated responses showed a consistent but not constant pattern in Figs. 6, 10, 13, 16, and 19 even in regions with a strong effect of backgrounds. Scaling of the first kind is not found for hadronic continuum spectra on carbon since the responses are not independent of momentum transfer. The hadron data do show a consistent scaling pattern of q dependence, not varying with beam species or beam energy.

Scaling of the second kind in electron scattering is defined as a finding of consistent responses from any nucleus, and is not addressed in this paper for hadrons, restricted to one nuclear sample. Scaling of the second kind for hadrons has been addressed for y scaling [35] and Bjorken scaling [39].

The range of hadron species available across a range of angles allowed the discovery of scaling of the third kind, independent of beam, at least for a restricted range of momentum transfers on one nucleus. This scaling was found to be closely followed for momentum transfers near 500 MeV/c on carbon in each of the five scaling systems as seen in Figs. 4, 9, 12, 15, and 18. The evolution of scaling responses at fixed values of each scaling variable was also much the same for each system, although with a very limited range in the Nachtmann variable. This Nachtmann variable does not bring agreement among hadronic continuum spectra as noted in Fig. 14. The averages of scaling responses in four of the systems near $q = 500$ MeV/c found these to be consistent within the accuracy expected from the use of data from several experiments. Scaling of this third kind is valid for hadrons over a relevant but limited kinematic range.

The dependence on momentum transfer (Table II) found the four systems other than the Nachtmann to yield consistent patterns but not constant with q. Overall, the y and ψ systems give the best unification, but the West and Bjorken systems are also adequate. The y-scaling responses were used as the examples in Sec. VIII. These judgments do depend upon the energy loss of the reaction.

There could be kinematic limits on the validity of scaling in beam energy (to meet the quasifree conditions both before and after the collision), momentum transfer (to avoid collective effects and to meet the quasifree conditions), and angle (to allow use of the Glauber model for determining the number of one-and-only-one beam-nucleon collisions). To achieve the momentum transfer standard, low-energy beams require large

scattering angles, and Fig. 3 shows that 392 MeV protons observed at 75° agree with the other responses only for low energy losses. At 18.3 GeV, inclusive proton spectra at moderate momentum transfers are driven by multistep processes [14,35,53]. The range of proton beam energies between 1014 MeV and 18.3 GeV has not been investigated for a carbon sample. Figure 20 shows that responses interpolated for fixed y vary little with beam energy for momentum transfers q near 500 MeV/c.

Scaling in the four appropriate scaling systems is most closely noted at low energy losses ω as in many of the preceding figures. This is the region of the responses furthest from pion production and other backgrounds and the most interesting in that these events are driven by the high-momentum components of the nuclear-momentum distribution. Figure 23 shows that, despite numerical instabilities, all hadrons do give much the same view of this distribution.

The validity of scaling as the momentum transfer q increases is judged by the agreement among the data cases as in Figs. 6, 10, 13, and 19. The effect of the isoscalar coupling to isoscalar responses is not noted in comparing Figs. 21 and 22, and the scatter of responses is greater for the three beam species and range of energies at $q = 350$ MeV/c than at $q = 500$ MeV/c seen in Fig. 4. The hope of using hadronic responses to measure isoscalar effects in nuclei is not met in the beam-energy range of this paper.

The successes of scaling agreements for four systems to organize continuum hadron scattering from carbon are noted, at least for some kinematic range, despite the conditions required to meet the terms of those models. Data at higher beam energies would do much to expand the reach of this paper, which found surprising agreement between simple pictures and complex reactions.

Recent efforts have demonstrated that theoretical methods can reproduce at least one example of hadron-nucleus continuum spectra, including spin observables [58]; it is to be hoped that such methods can lead to general insight from hadron beams as successful as those for electrons [59] and can account for the many simplicities noted in this present paper.

ACKNOWLEDGMENTS

Professor Y. Fujii and J. D. Zumbro provided most useful tables of data for this paper, and Salah E. Salah is thanked for valuable help with the many figures in this paper. This work was supported in part by the USDOE.

[1] D. B. Day, J. S. McCarthy, T. W. Donnelly, and I. Sick, Annu. Rev. Nucl. Part. Sci. **40**, 357 (1990).
[2] M. L. Goldberger and K. M. Watson, *Collision Theory* (Wiley, New York, 1964).
[3] T. Shigehara, K. Shimizu, and A. Arima, Nucl. Phys. A **492**, 388 (1989).
[4] J. D. Zumbro *et al.*, Phys. Rev. Lett. **71**, 1796 (1993).
[5] Y. Fujii *et al.*, Phys. Rev. C **64**, 034608 (2001).
[6] C. M. Kormanyos *et al.*, Phys. Rev. C **51**, 669 (1995).
[7] T. Kin *et al.*, Phys. Rev. C **72**, 014606 (2005).
[8] H. Esbensen and G. F. Bertsch, Phys. Rev. C **34**, 1419 (1986).
[9] H. Otsu, Ph.D. thesis, University of Tokyo, 1995.
[10] C. Chan *et al.*, Nucl. Phys. A **510**, 713 (1990).
[11] S. M. Beck and C. A. Powell, NASA Technical Report No. D-8119, 1976 (unpublished).
[12] R. E. Chrien *et al.*, Phys. Rev. C **21**, 1014 (1980).
[13] D. M. Corley *et al.*, Nucl. Phys. A **184**, 437 (1972).
[14] A. Klovning, O. Kofoed-Hansen, and K. Schlupmann, Nucl. Phys. B **54**, 29 (1973).
[15] D. Papadopoulou, Phys. Rev. C **65**, 054603 (2002).
[16] G. B. West, Phys. Rep. **18**, 263 (1975).
[17] G. F. Bertsch and O. Scholten, Phys. Rev. C **25**, 804 (1982).
[18] C. Maieron, T. W. Donnelly, and I. Sick, Phys. Rev. C **65**, 025502 (2002).
[19] Q. Ingram, E. Boshitz, L. Plug, J. Zichy, and J. P. Albanese, Phys. Lett. B **76**, 173 (1978).
[20] J. Ouyang, S. Hoibraten, and R. J. Peterson, Phys. Rev. C **47**, 2809 (1993).
[21] J. D. Patterson and R. J. Peterson, Nucl. Phys. A **717**, 235 (2003).
[22] [http://gwdac.physics.gwu.edu/].
[23] R. J. Peterson, Nucl. Phys. A **740**, 119 (2004).
[24] R. D. Smith and M. Bozoian, Phys. Rev. C **39**, 1751 (1989).
[25] C. Amsler *et al.*, Phys. Lett. B **667**, 1 (2008).
[26] R. Weiss *et al.*, Phys. Rev. C **49**, 2569 (1994).
[27] P. Lava, M. C. Martinez, J. Ryckebusch, J. A. Caballero, and J. M. Udias, Phys. Lett. B **595**, 177 (2004).
[28] S. A. Gurvitz, Phys. Rev. C **33**, 422 (1986).
[29] R. J. Peterson, Nucl. Sci. Eng. **161**, 346 (2009).
[30] R. J. Peterson, Few-Body Syst., Suppl. **9**, 17 (1995).
[31] H. Uberall, *Electron Scattering from Complex Nuclei* (Academic, New York/London, 1971).
[32] D. Abbott *et al.*, Phys. Rev. Lett. **80**, 5072 (1998).
[33] D. B. Day *et al.*, Phys. Rev. Lett. **59**, 427 (1987).
[34] T. W. Donnelly and I. Sick, Phys. Rev. C **60**, 065502 (1999).
[35] R. J. Peterson, Nucl. Phys. A **769**, 95 (2006).
[36] G. B. West, in *Momentum Distributions*, edited by R. N. Silver and P. E. Sokol (Plenum, New York/ London, 1989).
[37] B. W. Filippone *et al.*, Phys. Rev. C **45**, 1582 (1992).
[38] CLAS Collaboration, K. S. Egiyan *et al.*, Phys. Rev. C **68**, 014313 (2003); Phys. Rev. Lett. **96**, 082501 (2006).
[39] R. J. Peterson, Nucl. Phys. A **791**, 84 (2007).
[40] J. Arrington *et al.*, Phys. Rev. C **64**, 014602 (2001).
[41] M. B. Barbaro, R. Cenni, A. De Pace, T. W. Donnelly and A. Molinari, Nucl. Phys. A **643**, 137 (1998).
[42] A. N. Antonov, M. K. Gaidarov, D. N. Kadrev, M. V. Ivanov, E. M. de Guerra, and J. M. Udias, Phys. Rev. C **69**, 044321 (2004).
[43] A. N. Antonov, M. K. Gaidarov, M. V. Ivanov, D. N. Kadrev, E. Moya de Guerra, P. Sarriguren, and J. M. Udias, Phys. Rev C **71**, 014317 (2005).
[44] A. N. Antonov, M. V. Ivanov, M. K. Gaidarov, E. Moya de Guerra, P. Sarriguren, and J. M. Udias, Phys. Rev. C **73**, 047302 (2006).
[45] A. N. Antonov, M. V. Ivanov, M. B. Barbaro, J. A. Caballero, and E. M. de Guerra, Phys. Rev. C **79**, 044602 (2009).

[46] L. B. Rees, J. M. Moss, T. A. Carey, K. W. Jones, J. B. McClelland, N. Tanaka, A. D. Bacher, and H. Esbensen, Phys. Rev. C **34**, 627 (1986).
[47] X. Y. Chen *et al*., Phys. Rev. C **47**, 2159 (1993).
[48] T. N. Taddeucci *et al*., Phys. Rev. Lett. **73**, 3516 (1994).
[49] J. E. Wise *et al*., Phys. Rev. C **48**, 1840 (1993).
[50] Y. Fujii, Ph.D. thesis, Tohoku University, 1998.
[51] J. W. Lightbody and J. S. O'Connell, Computers in Physics **2**, 57 (1988).
[52] D. Day and I. Sick, Phys. Rev. C **69**, 028501 (2004).
[53] O. Kofoed-Hansen, Nucl. Phys. B **54**, 42 (1973).
[54] J. M. Finn, R. W. Lourie, and B. H. Cottman, Phys. Rev. C **29**, 2230 (1984).
[55] J. Bystricky, F. Lehar, and P. Winternitz, J. Phys. (Paris) **39**, 1 (1978).
[56] L. Ray, Phys. Rev. C **41**, 2816 (1990).
[57] A. Bodek and J. L. Ritchie, Phys. Rev. D **23**, 1070 (1981).
[58] D. D. van Niekerk, B. I. S. van der Ventel, N. P. Titus, and G. C. Hillhouse, Phys. Rev. C **83**, 044607 (2011).
[59] A. N. Antonov, M. V. Ivanov, J. A. Caballero, M. B. Barbaro, J. M. Udias, E. Moya de Guerra, and T. W. Donnelly, Phys. Rev. C **83**, 045504 (2011).